Commun Nonlinear Sci Numer Simulat 16 (2011) 2160–2168

Contents lists available at ScienceDirect

Commun Nonlinear Sci Numer Simulat

journal homepage: www.elsevier.com/locate/cnsns

Stick balancing with reflex delay in case of parametric forcing

Tamas Insperger *

Department of Applied Mechanics, Budapest University of Technology and Economics, H-1521 Budapest, Hungary

ARTICLE INFO

Article history:
Received 8 March 2010
Accepted 28 July 2010
Available online 2 August 2010

Keywords:
Time-delay
Stability
Semi-discretization
Inverted pendulum

ABSTRACT

The effect of parametric forcing on a PD control of an inverted pendulum is analyzed in the presence of feedback delay. The stability of the time-periodic and time-delayed system is determined numerically using the first-order semi-discretization method in the 5-dimensional parameter space of the pendulum's length, the forcing frequency, the forcing amplitude, the proportional and the differential gains. It is shown that the critical length of the pendulum (that can just be balanced against the time-delay) can significantly be decreased by parametric forcing even if the maximum forcing acceleration is limited. The numerical analysis showed that the critical stick length about 30 cm corresponding to the unforced system with reflex delay 0.1 s can be decreased to 18 cm with keeping maximum acceleration below the gravitational acceleration.

1. Introduction

Balancing of an inverted pendulum in the presence of feedback delay is an often referred example in dynamics and control theory [1–3] and it is also a relevant issue to human motion control [4–6]. It is known that conventional PD controllers cannot stabilize the upward position if the time delay is larger than a critical value. As it was shown by Stepan [7], this critical delay for a continuous PD feedback can be given in the simple form $\tau_{cr} = T/(\pi\sqrt{2})$, where T is the period of the small oscillations of the pendulum hanging at its downward position. The same phenomenon is often communicated such that for a given feedback delay, there is a critical minimum length of the pendulum: if the pendulum is shorter then this critical length, then the upward position is unstable for any PD controller [8].

Although, in most practical cases, the feedback delay cannot be eliminated from the system, its destabilizing effect can be abated by different control strategies. One technique to deal with the problem is the intermittent predictive controller [9], where the sequence of open-loop trajectories is punctuated by intermittent feedback. Another approach is the act-and-wait controller that is a special case of periodic controllers: the feedback term is switched off and on periodically [10]. Both the intermittent predictive controller and the act-and-wait controller have a generalized hold interpretation [11] and may be relevant to human motion control due to their intermittent nature [6,12,13].

A well known way for stabilizing unstable systems is parametric forcing: the upward position of a pendulum can be stabilized without any feedback control by vertically oscillating its suspension point [14,15]. The underlying mathematical model is the Mathieu equation, for which the stability properties are described by the celebrated Strutt–Ince diagram [16]. If parametric forcing is combined with delayed feedback, then the resulting mathematical model is a delayed-differential equation with time-periodic coefficients. Stability analysis for such systems is not trivial, but there exist several numerical methods to treat the problem (see for instance, [17–21]). A paradigm for time-delayed time-periodic systems is the delayed Mathieu equation [22].

* Tel.: +36 01 463 1227; fax: +36 01 463 3471.
E-mail address: inspi@mm.bme.hu

1007-5704/$ - see front matter © 2010 Elsevier B.V. All rights reserved.
doi:10.1016/j.cnsns.2010.07.025

The goal of this paper is to analyze the effect of parametric forcing on the stabilization of an inverted pendulum by PD control with delayed feedback. The paper was motivated by the work of Milton et al. [23], who analyzed human's stick balancing abilities when standing on a vibrating platform. This paper presents a numerical study on the problem. Stability properties are analyzed as function of the pendulum length, the control gains, the frequency and the amplitude of the parametric forcing. Stability is determined using the first-order semi-disretization method [24,25]. The outline of the paper is as follows. First the mechanical model is introduced in Section 2. Then, some special cases are considered in Section 3. Section 4 presents the semi-discretization algorithm to the stability analysis of the system. Section 5 deals with the analysis of the critical length for different forcing frequencies and amplitudes. The results are concluded in Section 6.

2. Mechanical model

The mechanical model under study is shown in Fig. 1. The stick is attached to the horizontal slide that moves periodically up and down together with the base according to the geometric constraint $r\cos(\omega t)$. The stick to be balanced is assumed to be homogeneous, its mass is m and its length is l. The mass m_0 of the slide is assumed to be negligible relative to the mass of the stick. The general coordinates are the angular position φ of the stick and the position x of the pivot point. A control force Q is applied on the slide in order to balance the stick. The equation of motion for the dynamic system takes the form

$$\begin{pmatrix} \frac{1}{3}ml^2 & \frac{1}{2}ml\cos\varphi \\ \frac{1}{2}ml\cos\varphi & m \end{pmatrix}\begin{pmatrix} \ddot{\varphi} \\ \ddot{x} \end{pmatrix} + \begin{pmatrix} \left(-\frac{1}{2}mgl + \frac{1}{2}mlr\omega^2\cos(\omega t)\right)\sin\varphi \\ -\frac{1}{2}ml\dot{\varphi}^2\sin\varphi \end{pmatrix} = \begin{pmatrix} 0 \\ Q(\varphi,\dot{\varphi}) \end{pmatrix}. \tag{1}$$

The displacement x is a cyclic coordinate that can be eliminated from the equation. The essential motion φ is then governed by

$$\left(\frac{1}{3}ml^2 - \frac{1}{4}ml^2\cos^2\varphi\right)\ddot{\varphi} + \frac{1}{8}ml^2\dot{\varphi}^2\sin 2\varphi + \left(-\frac{1}{2}mgl + \frac{1}{2}mlr\omega^2\cos\omega t\right)\sin\varphi = -\frac{1}{2}lQ(\varphi,\dot{\varphi})\cos\varphi. \tag{2}$$

The control force Q is assumed to be a locally linear function of the angular position φ and the angular velocity $\dot{\varphi}$ in the form

$$Q(\varphi,\dot{\varphi}) = P\varphi + D\dot{\varphi} + h.o.t., \tag{3}$$

where P is the proportional gain, D is the derivative gain and h.o.t. stands for the higher-order terms not modeled here.

Linearization around the upright position $\varphi = 0$ and modeling the delay τ in the feedback loop gives

$$\frac{1}{12}ml^2\ddot{\varphi}(t) + \left(-\frac{1}{2}mgl + \frac{1}{2}mlr\omega^2\cos\omega t\right)\varphi(t) = -\frac{1}{2}l(P\varphi(t-\tau) + D\dot{\varphi}(t-\tau)). \tag{4}$$

Introducing new parameters, the system can be transformed to the form

$$\ddot{\varphi}(t) + (-a + \varepsilon\cos\omega t)\varphi(t) = -p\varphi(t-\tau) - d\dot{\varphi}(t-\tau), \tag{5}$$

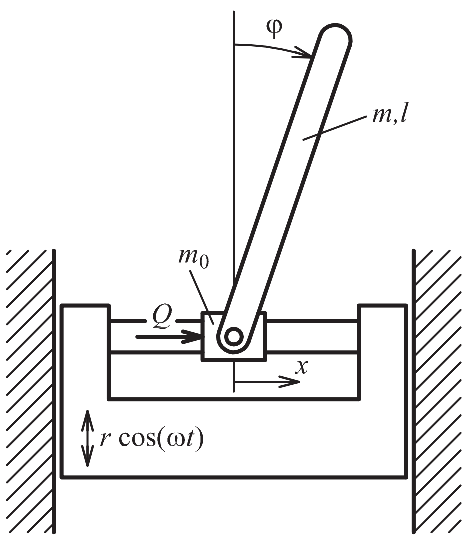

Fig. 1. Mechanical model of stick balancing with parametric excitation.

where

$$a = \frac{6g}{l}, \quad \varepsilon = \frac{6r\omega^2}{l}, \quad p = \frac{6P}{ml}, \quad d = \frac{6D}{ml}. \tag{6}$$

3. Special cases: *p* = 0, *d* = 0 and ε = 0

Eq. (5) covers two special cases: (1) when the controller is switched off, i.e., $p = 0$ and $d = 0$; (2) when there is no parametric forcing, i.e., $r = 0$ or $\varepsilon = 0$.

Case (1): If $p = 0$ and $d = 0$, then one obtain the classical Mathieu equation that describes the behavior of a pendulum under parametric forcing around the upward and the downward position. The stability diagram in the plane (a, ε), the so-called Strutt–Ince diagram [16], can be seen in the left panel of Fig. 2. The case $a < 0$ corresponds to the downward position of the pendulum, while the case $a > 0$ corresponds to the upward position (inverted pendulum).

The diagram in the right panel of Fig. 2 presents the stability domains transformed to the plane of the forcing frequency $f = \omega/(2\pi)$ and the forcing amplitude r for a pendulum of length $l = 50$ cm. The case when the maximum acceleration of the pivot point is equal to the gravitational acceleration g is denoted by dashed line. The stable domains are located above this limit, i.e., the upward position of the pendulum can only be stabilized by parametric forcing if the maximum acceleration exceeds g.

Case (2): If the amplitude of the parametric forcing is equal to zero then one get the governing equation for the PD control of an inverted pendulum with delayed feedback. The stability properties of this system are well known (see, for instance [1,26]). The stable domains in the plane of the control gains p and d are bounded by the line $p = a$ and the parametric curve

$$p = (\omega^2 + a)\cos(\omega t), \quad d = \frac{\omega^2 + a}{\omega}\sin(\omega t), \quad \omega \geqslant 0. \tag{7}$$

The corresponding stability diagrams can be seen in Fig. 3 for feedback delay $\tau = 0.1$ s and for different lengths l. The numbers in the diagrams denote the number of unstable roots (i.e., roots with positive real part). In the stable domains, this number is 0. It is known that the stable domain shrinks with increasing length l, and it disappears if $l > l_{crit,0} = 3g\tau^2$ [1,26]. For a feedback delay $\tau = 0.1$ s, a pendulum of length less than $l_{crit,0} = 0.2943$ m ≈ 30 cm cannot be balanced in its upward position using a traditional PD controller.

4. Stability analysis by semi-discretization

Stability analysis of Eq. (5) is performed using the semi-discretization method. The point of the method is that the delayed terms are discretized while the undelayed terms are unchanged and the time-periodic coefficients are approximated by piecewise constant functions. This way, the system is approximated by an ordinary differential equation (ODE) over each discretization interval. If the delayed terms are approximated by constants, then the method is called zeroth-order, if the they are approximated by linear function of time, then it is called first-order semi-discretization. The zeroth-order method was introduced in [17] for general delayed systems including time-dependent distributed time-delays. The first- and higher-order methods for the point delay case were presented in [25,24]. As it was shown in [24], if the time-periodic coefficients are approximated by piecewise constant functions, then second- or higher-order approximation of the delayed term does not yield any improvement in the convergence compared to the first-order approximation. A continuous time approximation

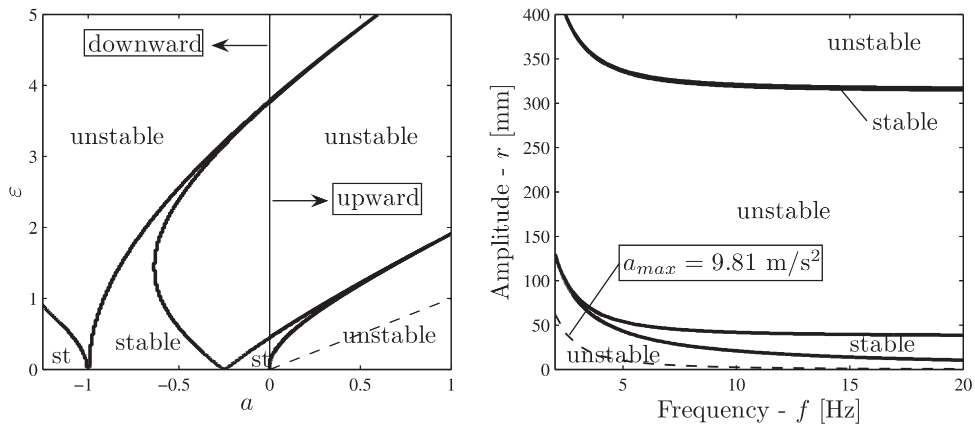

Fig. 2. Stability diagram for Eq. (5) with $p = 0$ and $d = 0$ in the plane (a, ε) (left) and in the plane of the forcing frequency f and amplitude r for a pendulum of length $l = 50$ cm (right). Dashed lines denotes the parameters where the maximum acceleration of the pivot point is equal to g.

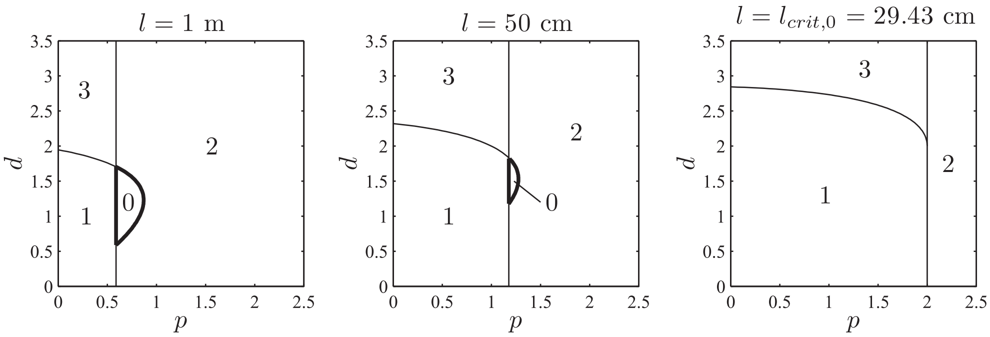

Fig. 3. Number of unstable roots for Eq. (5) with $\varepsilon = 0$ for feedback delay $\tau = 0.1$ s and for different lengths l.

technique was introduced in [27,28] based on the concept of semi-discretization that can handle multiple time-delays for both linear and nonlinear dynamical systems.

Here, the first-order semi-discretization method is used to determine the stability for Eq. (5). The steps of the method are briefly presented below. First, the system is transformed to the form

$$\dot{y}(t) = A(t)y(t) + Bu(t-\tau), \tag{8}$$
$$u(t) = Dy(t), \tag{9}$$

where

$$y = \begin{pmatrix} \varphi \\ \dot{\varphi} \end{pmatrix}, \quad A(t) = \begin{pmatrix} 0 & 1 \\ a - \varepsilon\cos(\omega t) & 0 \end{pmatrix}, \quad B = \begin{pmatrix} 0 \\ 1 \end{pmatrix}, \quad D = (\,-p \;\; -d\,). \tag{10}$$

Then, the discretization time step $h = T/k$ is introduced, where $k \in Z^+$. The system is approximated as

$$\dot{\tilde{y}}(t) = \widetilde{A}_i\tilde{y}(t) + B(\beta_1(t)\tilde{u}_{i+1-n} + \beta_0(t)\tilde{u}_{i-n}), \quad t \in [ih, (i+1)h), \tag{11}$$
$$\tilde{u}_i = \tilde{u}(ih) = D\tilde{y}(ih), \tag{12}$$

where

$$\widetilde{A}_i = \frac{1}{h}\int_{ih}^{(i+1)h} A(t)dt, \quad i \in \mathbb{Z}, \tag{13}$$
$$\beta_1(t) = \frac{t-\tau-(i-n)h}{h}, \quad \beta_0(t) = -\frac{t-\tau-(i+1-n)h}{h} \tag{14}$$

and $n = \mathrm{int}(\tau/h + 1/2)$. Note that the approximation parameter is the number k of discretization intervals over the period T, and number n (the delay parameter) is defined such that $(n+1/2)h \approx \tau$. Eqs. 11 and 12 define an ordinary differential equation with piecewise linear forcing that can be solved step-by-step over each discretization interval in the form

$$\tilde{y}_{i+1} = \tilde{y}((i+1)h) = P_i\tilde{y}(ih) + R_{i,0}\tilde{u}_{i-n} + R_{i,1}\tilde{u}_{i+1-n}, \tag{15}$$

where

$$P_i = \mathrm{e}^{\widetilde{A_i(h)}}, \tag{16}$$
$$R_{i,0} = -\int_0^h \frac{s-\tau+(n-1)h}{h}\mathrm{e}^{\widetilde{A}_i(h-s)}B\,\mathrm{d}s, \tag{17}$$
$$R_{i,1} = \int_0^h \frac{s-\tau+nh}{h}\mathrm{e}^{\widetilde{A}_i(h-s)}B\,\mathrm{d}s. \tag{18}$$

If $\tilde{A}_i^{-1}$ exists, then integration gives

$$R_{i,0} = \left(\widetilde{A}_i^{-1} + \frac{1}{h}\left(\widetilde{A}_i^{-2} - (\tau-(n-1)h)\widetilde{A}_i^{-1}\right)\left(I - \mathrm{e}^{\widetilde{A}_i h}\right)\right)B, \tag{19}$$
$$R_{i,1} = \left(-\widetilde{A}_i^{-1} + \frac{1}{h}\left(-\widetilde{A}_i^{-2} + (\tau-nh)\widetilde{A}_i^{-1}\right)\left(I - \mathrm{e}^{\widetilde{A}_i h}\right)\right)B. \tag{20}$$

Eqs. 15 and 12 implies the $(n+2)$-dimensional discrete map

$$z_{i+1} = C_i z_i \tag{21}$$

with

$$z_i = \begin{pmatrix} \tilde{y}_i \\ \tilde{u}_{i-1} \\ \tilde{u}_{i-2} \\ \vdots \\ \tilde{u}_{i-n} \end{pmatrix}, \qquad C_i = \begin{pmatrix} P_i & 0 & \dots & 0 & R_{i,1} & R_{i,0} \\ D & 0 & \dots & 0 & 0 & 0 \\ 0 & I & \dots & 0 & 0 & 0 \\ \vdots & & & & \vdots & \vdots \\ 0 & 0 & \dots & 0 & I & 0 \end{pmatrix}. \tag{22}$$

Multiple recursive applications of Eq. (21) with initial state z_0 gives the monodromy mapping

$$z_k = \Phi z_0 \tag{23}$$

with

$$\Phi = C_{k-1} C_{k-2} \dots C_0 \tag{24}$$

that is a finite dimensional approximation of the infinite dimensional monodromy operator of the original system (8) and (9). The system is asymptotically stable if all the eigenvalues of the monodromy matrix are located within the unit circle of the complex plane.

Fig. 4 presents some sample stability diagrams in the plane (p,d) for a stick of length $l = 50$ cm with forcing amplitude $r = 5$ mm and forcing frequencies $f = 2$, 2.5 and 3 Hz. The diagrams were determined via point-by-point evaluation of the critical eigenvalues over a 100×100-sized grid of parameters p and d. The approximation parameter was $k = 25$, 20 and 17 for the cases $f = 2$, 2.5 and 3 Hz, respectively. The corresponding delay parameter was $n = 5$ for all cases. It can be seen that the stability diagrams qualitatively differ from the ones of the time-invariant system with $\varepsilon = 0$. Here, the stable domains are serrated by unstable tongues caused by the parametric forcing. Note that Eq. (5) was also analyzed in [29], where similar stability diagrams were presented in the plane (p,d), while the same system under PI control was analyzed in [30].

5. Effect of parametric forcing on the critical stick length

The goal of this study is to analyze the effect of parametric forcing on the stabilization process. Stability charts in the plane (p,d) are therefore determined for a series of forcing frequencies f, forcing amplitudes r and pendulum lengths l. As a first step, a set of diagrams is presented in Fig. 5 that describes the changes in the stability properties for different f, r and l. Different colors denote stability boundaries for different lengths l, while the feedback delay is $\tau = 0.1$ s for all plots. The approximation parameter was determined such that $k \geqslant 10$ and $n \geqslant 5$. It can be seen that for small amplitudes and for small frequencies, stable domains arise only for the lengths $l = 40$, 60, 80 and 100 cm that are all larger then the critical length $l_{crit,0} = 30$ cm for the unforced system. For large amplitudes and large frequencies, stable domains arise also for the case $l = 20$ cm (see, for instance the case $r = 20$ mm with $f = 6$ Hz, where the boundaries for all lengths can clearly be seen).

Fig. 6 presents the critical stick lengths for different forcing frequencies and amplitudes. The chart was determined in the following way. The frequency and amplitude were changed between 2 and 20 Hz and 0 and 10 mm, respectively, both in 100 steps providing a 100×100 grid over the plane (f,r). For each pair (f,r), the length was fixed to a starting value of $l_{\text{start}} = 5$ cm, and the stability diagrams were determined over a 100×100 grid in the plane (p,d) with the bounds $-0.5 \leqslant p \leqslant 2$ and $-0.5 \leqslant d \leqslant 2$ (as in Fig. 5). Then the length of the stick was increased by $\Delta l = 2.5$ cm, and the stability diagram was computed again. The process was repeated until no stable region was found within the region $-0.5 \leqslant p \leqslant 2$, $-0.5 \leqslant d \leqslant 2$. The corresponding length was denoted as the critical length for the pair (f,r). The approximation parameter for the first-order semi-discretization method was such that $k \geqslant 10$ and $n \geqslant 5$. The calculation process was strongly time-consuming, since the critical eigenvalue had to be calculated for around 8.5×10^8 different parameter combinations (for 100×100 grid over the (p,d) plane, for 100×100 grid over the (f,r) plane and for an average 8.5 different lengths l). The calculation of the diagram in Fig. 6 took 16 days on a normal notebook (Intel Core 2 Duo Processor, 2.4 GHz, 2 GB).

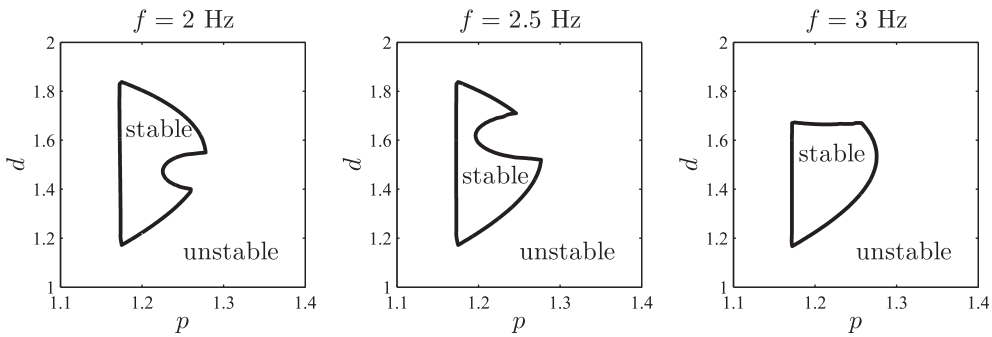

Fig. 4. Stability charts for Eq. (5) with feedback delay $\tau = 0.1$ s, stick length $l = 50$ cm, forcing amplitude $r = 5$ mm for different forcing frequencies f.

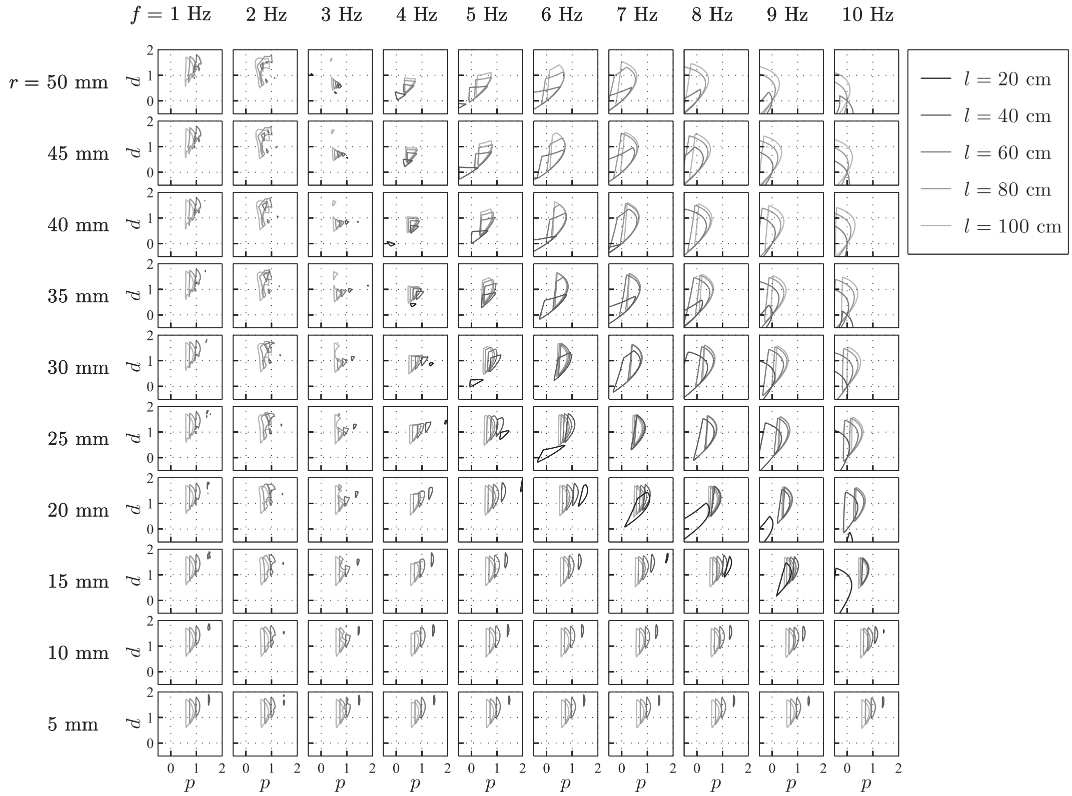

Fig. 5. Set of stability charts for Eq. (5) with τ = 0.1 s for different forcing frequencies f and amplitudes r. Different lengths are denoted by different colors (see the legend on the right). For large amplitudes and large frequencies, the stable regions appears also for length l = 20 cm.

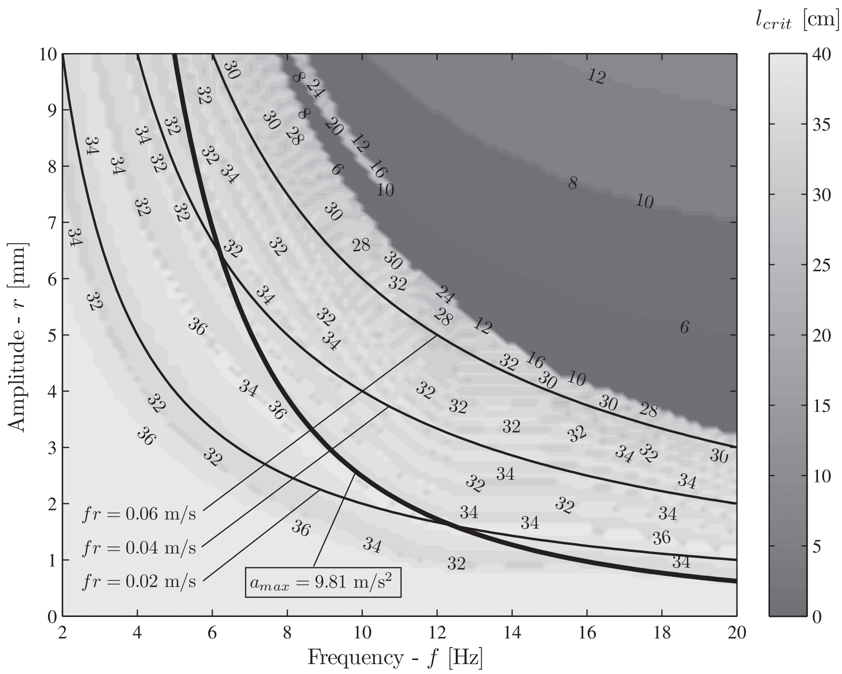

Fig. 6. Color map for the critical length as function of forcing frequency and amplitude for τ = 0.1 s. Numbers denote the critical lengths. Thin lines denote the hyperbola $f\,r$ = 0.02, 0.04, 0.06 m/s. Thick line corresponds to the case when the maximal acceleration equals to g.

The color-bar in Fig. 6 denotes the critical stick length l_{crit}. Some values are also presented in the main diagram in order to help to identify the corresponding colors. During the analysis of the diagram, it should be considered that the stability diagrams were determined numerically at discrete pairs (f,r) with discrete lengths l in the (p,d) plane with $-0.5 \leqslant p \leqslant 2$, $-0.5 \leqslant d \leqslant 2$. This is the reason for the fragmented contour lines. It can be seen that for the case, when the forcing amplitude is zero, the critical stick length is about $36 \sim 38$ cm that is larger then the theoretical value $l_{crit,0} = 30$ cm for the unforced system. This is again due to the discrete numerical analysis of the parameter domains: the 100×100 resolution over the parameter plane (p,d) is not fine enough to find the very narrow stability regions for lengths close to l_{crit}.

In spite of the numerical fragmentation of the diagram, the tendency can clearly be seen: the critical length of the pendulum decreases for increasing f and r approximately along the hyperbola fr = const. Some of these hyperbola are presented in the figure for fr = 0.02, 0.04 and 0.06 m/s by thin lines for reference. A radical change in the critical length can be observed above the hyperbola fr = 0.06 m/s, were the critical length tends to the minimum starting value $l_{\text{start}} = 5$ cm. This result is not surprising, since it is known that an inverted pendulum of any length can be stabilized by appropriate (i.e., high enough) forcing frequency and forcing amplitude even without feedback control. However, if the power or the maximum acceleration of the forcing is limited, then the forcing frequency and the amplitude cannot be increased arbitrarily.

A relevant issue in human stick balancing is that the base of the stick is in contact with the fingertip that implies that the downward acceleration cannot exceed gravitational acceleration g, i.e. $a_{\max} = r\omega^2 \leqslant g$ (with $\omega = 2\pi f$).This limit is denoted by thick line in Fig. 6. It can be seen that the slope of this limit is larger then the slope of the fr = const hyperbola. This suggest that in case of human stick balancing, parametric forcing is more effective if the forcing frequency is relatively small, while the forcing amplitude is relatively large. Fig. 7 shows a similar plot for the parameters $2 \leqslant f \leqslant 20$ Hz and $0 \leqslant r \leqslant 50$ mm. It can be seen that the critical length goes below $0.24 \sim 0.26$ even if $a_{\max} \leqslant g$ (see around $f = 2 \sim 3$ Hz with $r = 30 \sim 40$ mm).

In order to confirm that a stick of length less than 30 cm can be balanced with reflex delay $\tau = 0.1$ s in case of parametric forcing, a detailed stability analysis is performed for $f = 2.5$ Hz with $r = 30$ mm. The corresponding maximal acceleration is $a_{\max} = 7.4$ m/s^2, i.e., the contact between the base of the stick and the fingertip is continuously maintained. The stability diagrams are presented in Fig. 8. It can be seen that very narrow stable domains do exist even for the length 18 cm. This means that stick balancing properties can be improved by parametric forcing even if the maximum acceleration of the stick's base does not exceeds gravitational acceleration g.

6. Conclusions

The effect of parametric forcing on a PD control of an inverted pendulum was analyzed in the presence of feedback delay. The stability of the time-periodic and time-delayed system was determined numerically using the first-order semi-discretization method in the 5-dimensional parameter space of the pendulum length, the forcing frequency, the forcing amplitude, the proportional and the differential gains. Due to the large number of parameters, the computations were time-consuming.

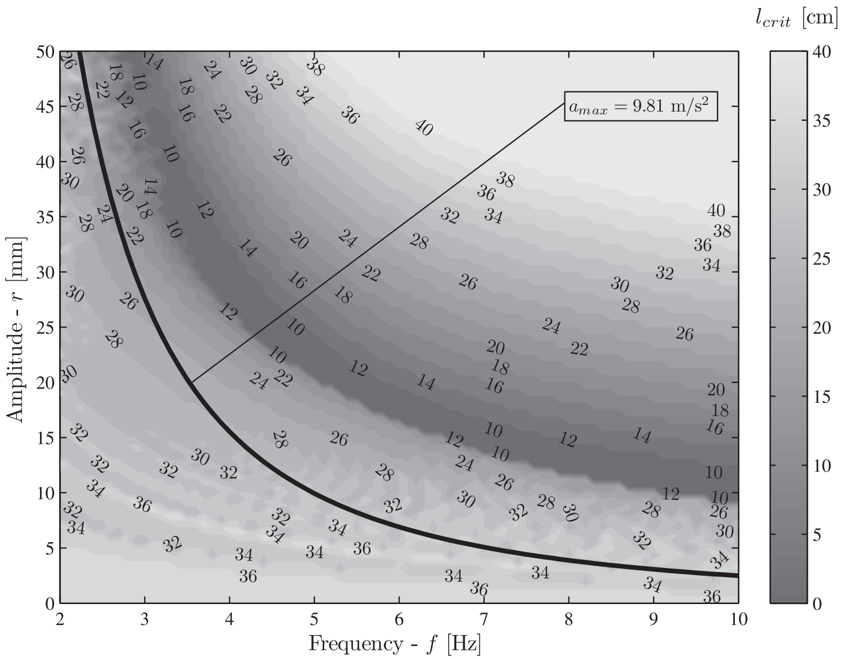

Fig. 7. Color map for the critical length as function of forcing frequency and amplitude for $\tau = 0.1$. Numbers denote the critical lengths. Thick line corresponds to the case when the maximal acceleration equals to g.

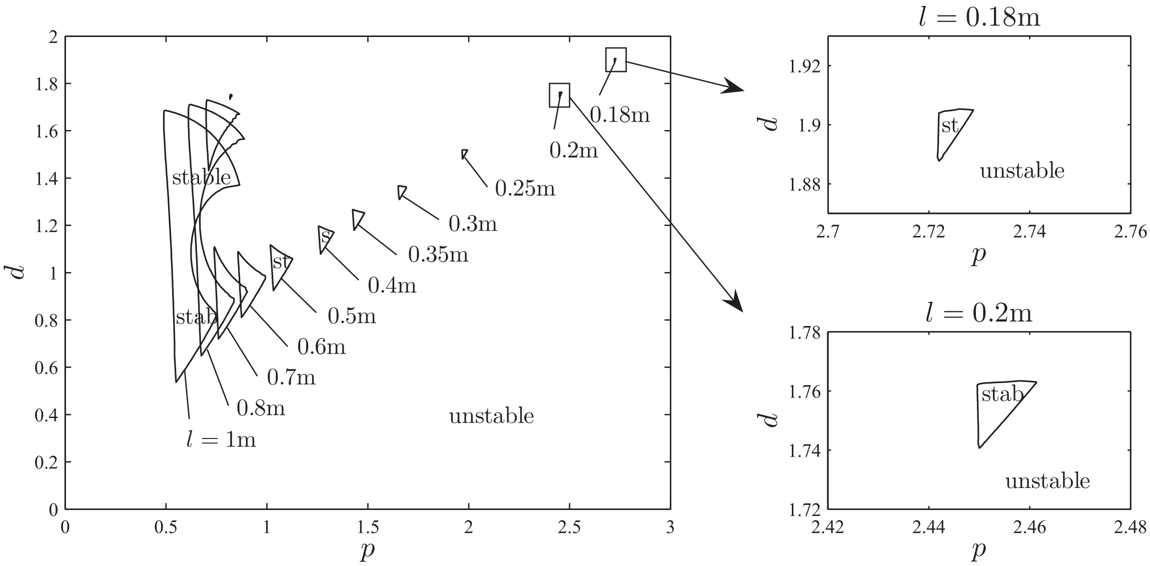

Fig. 8. Wandering of the stability boundaries in the plane (p, d) for forcing frequency $f = 2.5$ Hz and forcing amplitude $r = 30$ mm for different lengths l. The maximum acceleration is $a_{max} = 7.4$ m/s^2. Very narrow stable domains were found for length $l = 18$ cm.

The critical length of the pendulum (defined as the length that can just be balanced against the time-delay) was determined for different frequencies and amplitudes. For the case without parametric forcing, the critical length to a reflex delay of 0.1 s is about 30 cm. If there is no limitation to the forcing parameters, then the critical length can be decreased arbitrarily, since an inverted pendulum of any length can be stabilized by large enough forcing frequency and amplitude even without feedback control.

If the frequency and/or the amplitude of the parametric forcing are limited by any reason, then the critical length cannot be decreased arbitrarily. This issue is relevant to stick balancing at the fingertip [23], where the acceleration of the stick's base cannot exceed gravitational acceleration. The numerical study showed that the critical length can effectively be decreased for this case, too, with relatively low forcing frequencies (around $2 \sim 3$ Hz) and relatively large forcing amplitudes (around $3 \sim 4$ cm). For instance, the critical length to the reflex delay 0.1 s with frequency 2.5 Hz and amplitude 30 mm was found to be 18 cm.

In this analysis, the stick balancing ability was characterized by the stability of the process based on a purely mechanical model. This model provides information only about the existence of such control gains that provides a stable control process in the neighborhood of the upward position in the presence of given feedback delays. Other aspects, like the survival times [8,23], i.e., the time interval for that one is able to balance a stick at the fingertip, can hardly be evaluated based on this model. This phenomenon is rather related to a more complex model of the combined mechanical and neural system.

Acknowledgement

This research was supported in part by the János Bolyai Research Scholarship of the Hungarian Academy of Sciences, by the Hungarian National Science Foundation under Grant No. OTKA K72911.

References

[1] Stepan G. Retarded Dynamical Systems. Harlow: Longman; 1989.
[2] Sieber J, Krauskopf B. Complex balancing motions of an inverted pendulum subject to delayed feedback control. Physica D 2004;197:332–45.
[3] Landry M, Campbell SA, Morris K, Aguilar CO. Dynamics of an inverted pendulum with delayed feedback control. SIAM J. Applied Dynamical Systems 2005;4(2):333–51.
[4] Beamish D, Bhatti S, Wu JH, Jing ZJ. Performance limitations from delay in human and mechanical motor control. Biological Cybernetics 2008;99(1):43–61.
[5] Milton J, Cabrera JL, Ohira T, Tajima S, Tonosaki Y, Eurich CW, et al. The time-delayed inverted pendulum: implications for human balance control. Chaos 2009;19:026110.
[6] Asai Y, Tasaka Y, Nomura K, Nomura T, Casadio M, Morasso P. A model of postural control in quiet standing: robust compensation of delay-induced instability using intermittent activation of feedback control. PLoS ONE 2009;4(7):e6169.
[7] Stepan G. Delay effects in the human sensory system during balancing. Philosophical Transactions of The Royal Society A – Mathematical Physical and Engineering Sciences. 2007;367:1195–212.
[8] Cabrera JL, Milton JG. Stick balancing: on-off intermittency and survival times. Nonlinear Science 2004;11(3):305–17.
[9] Gawthrop PJ, Wang L. Intermittent model predictive control. Proceedings of the Institution of Mechanical Engineers Part I-Journal of Systems and Control Engineering 2007;221(7):1007–18.

[10] Insperger T. Act and wait concept for time-continuous control systems with feedback delay. IEEE Transactions on Control Systems Technology 2006;14(5):974–7.
[11] Gawthrop P. Act-and-wait and intermittent control: some comments. IEEE Transactions on Control Systems Technology 2009;PP(99):1–4.
[12] Milton J, Townsend JL, King MA, Ohira T. Balancing with positive feedback: the case for discontinuous control. Philosophical Transactions of the Royal Society of London Series A-Mathematical Physical and Engineering Sciences 2009;367:1181–93.
[13] Loram ID, Lakie M, Gawthrop PJ. Visual control of stable and unstable loads: what is the feedback delay and extent of linear time-invariant control? Journal of Physiology 2009;587(6):1343–65.
[14] Stephenson A. On a new type of dynamical stability. Memoirs and Proceedings of the Manchester Literary and Philosophical Society 1908;52:1–10.
[15] Levi M. Stability of the inverted pendulum a topological explanation. SIAM Review 1988;30(4):639–44.
[16] van der Pol F, Strutt MJO. On the stability of the solutions of Mathieu's equation. Philosophical Magazine, and Journal of Science 1928;5:18–38.
[17] Insperger T, Stepan G. Semi-discretization method for delayed systems. International Journal for Numerical Methods in Engineering 2002;55(5):503–18.
[18] Breda D, Maset S, Vermiglio R. Computing the characteristic roots for delay differential equations. IMA Journal of Numerical Analysis 2004;24(1):1–19.
[19] Butcher EA, Ma H, Bueler E, Averina V, Szabo Zs. Stability of time-periodic delay-differential equations via Chebyshev polynomials. International Journal for Numerical Methods in Engineering 2004;59(7):895–922.
[20] Szalai R, Stepan G, Hogan SJ. Continuation of bifurcations in periodic delay-differential equations using characteristic matrices. SIAM Journal on Scientific Computing 2006;28(4):1301–17.
[21] Mann BP, Patel BR. Stability of delay equations written as state space models. Journal of Vibration and Control 2010;16(7–8):1067–85.
[22] Insperger T, Stepan G. Stability chart for the delayed Mathieu equation. Proceedings of the Royal Society London A 2002;458:1989–98.
[23] Milton JG, Ohira T, Cabrera JL, Fraiser RM, Gyorffy JB, Ruiz FK, et al. Balancing with vibration: a prelude for "drift and act balance control. PLoS ONE 2009;4(10):1–11. art. no. e7427.
[24] Insperger T, Stepan G, Turi J. On the higher-order semi-discretizations for periodic delayed systems. Journal of Sound and Vibration 2008;313:334–41.
[25] Elbeyli O, Sun JQ. On the semi-discretization method for feedback control design of linear systems with time delay. Journal of Sound and Vibration 2004;273(1–2):429–40.
[26] Stepan G, Kollar L. Balancing with reflex delay. Mathematical and Computer Modelling 2000;31:199–205.
[27] Sun JQ. A method of continuous time approximation of delayed dynamical systems. Communications in Nonlinear Science and Numerical Simulation 2009;14:998–1007.
[28] Sun JQ, Song B. Control studies of time-delayed dynamical systems with the method of continuous time approximation. Communications in Nonlinear Science and Numerical Simulation 2009;14:3933–44.
[29] Sheng J, Elbeyli o, Sun JQ. Stability and optimal feedback controls for time-delayed linear periodic systems. AIAA Journal 2004;42(5):908–11.
[30] Sheng J, Sun JQ. Feedback controls and optimal gain design of delayed periodic linear systems. Journal of Vibration and Control 2005;11(2):277–94.